Low-Light-Induced Formation of Semicrystalline Photosystem II Arrays in Higher Plant Chloroplasts †

ARTICLE *in* BIOCHEMISTRY · NOVEMBER 2007

Impact Factor: 3.02 · DOI: 10.1021/bi700748y · Source: PubMed

6 AUTHORS, INCLUDING:

Helmut Kirchhoff
Washington State University
38 PUBLICATIONS **1,333** CITATIONS
SEE PROFILE

Ravi Danielsson
Malmö University
9 PUBLICATIONS **296** CITATIONS
SEE PROFILE

Per-Ake Albertsson
Lund University
30 PUBLICATIONS **748** CITATIONS
SEE PROFILE

Low-Light-Induced Formation of Semicrystalline Photosystem II Arrays in Higher Plant Chloroplasts†

Helmut Kirchhoff,*,‡ Winfried Haase,§ Sandra Wegner,‡ Ravi Danielsson,|| Ralf Ackermann,‡ and Per-Ake Albertsson||

Institute of Botany, Schlossgarten 3, D-48149 Münster, Germany, Max Planck Institute of Biophysics, Max-von-Laue Strasse 3, D-60438 Frankfurt a. M., Germany, and Department of Biochemistry, Lund University, P.O. Box 124, SE-221 00 Lund, Sweden

Received April 20, 2007; Revised Manuscript Received June 26, 2007

ABSTRACT: Remodeling of photosynthetic machinery induced by growing spinach plants under low light intensities reveals an up-regulation of light-harvesting complexes and down-regulation of photosystem II and cytochrome b_6f complexes in intact thylakoids and isolated grana membranes. The antenna size of PSII increased by 40−60% as estimated by fluorescence induction and LHCII/PSII stoichiometry. These low-light-induced changes in the protein composition were accompanied by the formation of ordered particle arrays in the exoplasmic fracture face in grana thylakoids detected by freeze-fracture electron microscopy. Most likely these highly ordered arrays consist of PSII complexes. A statistical analysis of the particles in these structures shows that the distance of neighboring complexes in the same row is 18.0 nm, the separation between two rows is 23.7 nm, and the angle between the particle axis and the row is 26°. On the basis of structural information on the photosystem II supercomplex, a model on the supramolecular arrangement was generated predicting that two neighboring complexes share a trimeric light-harvesting complex. It was suggested that the supramolecular reorganization in ordered arrays in low-light grana thylakoids is a strategy to overcome potential diffusion problems in this crowded membrane. Furthermore, the occurrence of a hexagonal phase of the lipid monogalactosyldiacylglycerol in grana membranes of low-light-adapted plants could trigger the rearrangement by changing the lateral membrane pressure.

Vascular plants live in an environment with high fluctuations in both light quantity and quality. The lack of their mobility and the need for optimizing light harvesting on variable light conditions led to the evolution of adaptation mechanisms of their photosynthetic machinery localized in the thylakoid membrane system of chloroplasts (*1*, *2*). This unique membrane is characterized by membrane stacks (grana thylakoids) which are interconnected by unstacked stroma lamellae (*3*). The energy-transforming machinery consists of five membrane-integral multisubunit protein complexes (PSII,[1] PSI, cytochrome b_6f complex, LHCII, and ATPase) which can form oligomers called supercomplexes: trimeric LHCII, PSI−LHCI tetramer, dimeric cytochrome b_6f complex, and dimeric LHCII trimer−PSII (*4*). These complexes are nonhomogenously distributed between stacked grana thyakoids (mainly PSII and LHCII complexes) and stroma lamellae (mainly PSI, LHCI, and ATPase) (*5*). Because on the molecular level even full sunlight is a diluted energy source (*6*), efficient light harvesting and lossless transformation of captured light quanta into NADPH and ATP are of utmost importance at low photon flux densities. In this respect a central adaptation strategy is the light-controlled dynamic remodeling of the protein composition in thylakoids which includes the down-regulation of the PSII, cytochrome b_6f complexes, and ATPase content and the up-regulation of LHCII (e.g., ref *7*). At the microscopic level, the size of grana stacks increases, i.e., the number of disks in each granum increases (*7*), while the proportion of stroma lamellae, i.e., the area of stroma lamellae as a percentage of the total thylakoid area, remains constant, about 20% (*8*). This leads to an improved light-harvesting function and a down-regulation of the electron transport function.

However, the consequences of the low-light-induced remodeling of the photosynthetic apparatus, i.e., the substitution of a fraction of relatively large PSII supercomplexes by smaller LHCII, on the supramolecular organization of protein complexes and their mobility and function are poorly understood. It is interesting that PSII supercomplexes in grana thylakoids have the potential to rearrange from a more or less random distribution to a highly ordered semicrystalline organization (see ref *9* for a recent review), which highlights the flexibility of the protein network. The functional significance of the rearrangement in highly ordered arrays is unknown. Evidence has accumulated that this could be

† H.K. is supported by the Deutsche Forschungsgemeinschaft and P.-A.A. by grants from the Royal Physiographic Society in Lund and the Carl Trygger Foundation.

* To whom correspondence should be addressed. Phone: +49 251 8324820. Fax: +49 251 8323823. E-mail: kirchhh@uni-muenster.de.

‡ Institute of Botany.

§ Max Planck Institute of Biophysics.

|| Lund University.

[1] Abbreviations: Chl, chlorophyll; EF, exoplasmic fracture face; F_v, variable chlorophyll *a* fluorescence; HII, inverted hexagonal phase of MGDG; LHC, light-harvesting complex; MGDG, monogalactosyldiacylglycerol; LL, low light; OL, ordinary light; PQ, plastoquinone; PF, protoplasmic fracture face; PS, photosystem; QA, primary chinon acceptor of photosystem II.

10.1021/bi700748y CCC: $37.00
Published on Web 09/11/2007

Table 1: Chlorophyll *a*/*b* Ratio and Content of Marker Redox Chromophores for Protein Complexes of Membranes Prepared from Plants Grown under Low (LL) and Ordinary (OL) Light Intensities[a]

	LL thylakoids	OL thylakoids	LL grana (B3)	OL grana (B3)
chlorophyll *a*/*b*	2.7 ± 0.1	3.0 ± 0.1	2.1 ± 0.1	2.4 ± 0.1
cytochrome b_{559}	2.52 ± 0.25	3.29 ± 0.33	3.07 ± 0.19	4.41 ± 0.23
P700	1.27 ± 0.12	1.31 ± 0.07	0.59 ± 0.03	0.61 ± 0.03
cytochrome *f*	0.90 ± 0.06	1.35 ± 0.03	0.96 ± 0.06	1.57 ± 0.05
cytochrome $b_6 \times 1/2$	0.94 ± 0.19	1.33 ± 0.05	0.99 ± 0.11	1.50 ± 0.25

[a] The values are the means of at least three independent determinations with standard deviations. The dimension, with the exception of the chlorophyll *a*/*b* ratio, is mmol/mol of chlorophyll. For a better comparison the values for cytochrome b_6 are divided by 2 because each cytochrome b_6f complex contains two b_6 molecules. Note the similarities of the cytochrome *f* and 1/2 cytochrome b_6 values, indicating the reliability of the fitting procedure.

correlated with a stress response of the plant (*9*), indicating that ordering of PSII into 2D crystals in grana thylakoids could be associated with an optimization of photosynthetic functions under suboptimal environmental conditions. In this study we examined the low-light-induced remodeling of the photosynthetic apparatus and correlated the alterations with changes in the PSII organization in grana thylakoids measured by freeze-fracture electron microscopy.

MATERIALS AND METHODS

Preparation of Thylakoid and Grana Membranes. Spinach (*Spinacia oleracia* L.) was grown hydroponically at 20 °C with a light period of 12 h and under cool white fluorescent light at an incident light intensity of 300 (OL) or 30 (LL) μmol of photons m^{-2} s^{-1}. Thylakoids, grana vesicles (B3), were isolated from exposed leaves by the batch procedure as described (*10*, *11*).

Spectroscopy. Cytochrome *f*, b_6, and b_{559} contents were determined from chemical difference absorption spectra measured between 520 and 580 nm (Hitachi U3010 spectrometer, spectral resolution 1 nm, scan speed 120 nm × min^{-1}, average of 10 scans) in the presence of 0.03% dodecyl β-maltoside as described previously (*12*). Cytochrome concentrations were calculated with difference absorption coefficients summarized in ref *12* or of 25.1 mM^{-1} cm^{-1} at 560 nm for cytochrome b_{559} as recently determined (*13*). The content of P700 was deduced from light pulse (200 ms, 6000 μmol of quanta m^{-2} s^{-1}) induced absorption changes at 810 nm − 860 nm in the presence of 0.2% dodecyl β-maltoside as recently described (*14*).

Chlorophyll *a* fluorescence induction kinetics were measured with a home-built apparatus as described in ref *15*. Isolated thylakoid membranes were incubated for at least 5 min in darkness in a buffer containing 7 mM $MgCl_2$, 40 mM KCl, 330 mM sorbitol, and 25 mM HEPES (pH 7.6, KOH) at a chlorophyll concentration of 10 μg mL^{-1}. One minute before the actinic light was switched on 20 μM DCMU was added. The data were analyzed with SigmaPlot version 8.0 (Jandel Scientific).

Electron Microscopy. A droplet of a dense membrane suspension placed in copper sample holders was frozen at −180 °C in liquefied ethane. Using a double-fracture device, the sample was then fractured in a BAF400T freeze-fracture machine (BalTec, Liechtenstein) and the platinum/carbon replicas were photographed in an EM208S electron microscope (FEI Co.).

Raw images were analyzed with a particle count routine (software OPTMAS 6.5). This routine finds particles which are higher than a given height threshold and fit each individual particle with an ellipse. The data of this fitting are shown in Figure 2A.

RESULTS

Characterization of Thylakoid and Grana Membranes Isolated from OL- and LL-Adapted Plants. Table 1 summarizes the chlorophyll *a*/*b* ratio and the content (relative to chlorophyll) of marker redox chromophores for PSII (cytochrome b_{559}), cytochrome b_6f complex (cytochrome *f* and b_6), and PSI (P700) in membranes isolated from OL- and LL-grown plants. The content of PSI is almost unchanged in thylakoids from LL plants. In contrast, the concentrations of both PSII and the cytochrome b_6f complex were reduced by about 30% in LL thylakoids. Furthermore, the decreased chlorophyll *a*/*b* ratio indicated an increased LHCII content. These low-light-induced changes are in good accordance with literature data (*1*, *2*, *8*, *16*). Changes similar to those for intact thylakoids were measured for isolated grana thylakoids (Table 1). Interestingly, the ratio of PSII to cytochrome b_6f complex is nearly unchanged in both intact thylakoids (2.7 for LL versus 2.5 for OL) and in isolated grana membranes (3.1 for LL versus 2.9 for OL), indicating the concerted regulation of the content of both protein complexes.

Because the content of PSII reaction centers (quantified by cytochrome b_{559}) in grana thylakoids of low-light-adapted plants decreased by about 30% (Table 1), it is likely that this corresponds to a decrease in the density of PSII complexes in this subcompartment. Testing this assumption, we analyzed the particle density in stacked membrane regions in electron microscopic micrographs of freeze-fractured intact thylakoids. Freeze-fracturing splits the membrane bilayer into two monolayers which are called EF (exoplasmic) and PF (protoplasmic) fracture faces and are further subdivided into EFs, EFu, PFs, and PFu ("s" for stacked and "u" for unstacked membrane regions). There is good evidence that PSII complexes are exposed exclusively in the EF half-membrane and all other complexes (including LHCII) in the PF half-membrane (*16*). The EFs face is easily identified by (i) its larger particle size and lower density compared to those of the PF face and (ii) by a higher density compared to that of the EFu region. Examples of EM micrographs of freeze-fracture LL and OL thylakoids are given in Figure 1. From a quantitative analysis of such micrographs (Table 2), it follows that the EFs particle density (per membrane area) in LL thylakoids is significantly (17%) lower, indicating that growing plants under low light leads to a dilution of PSII packing in accordance with the cytochrome b_{559} data (Table 1). An unexpected observation was the occurrence of highly

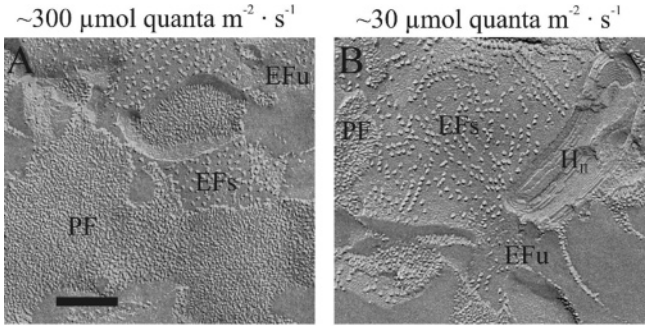

FIGURE 1: Electron micrograph of freeze-fracture thylakoid membranes: A, from OL-grown plants; B, from LL-grown plants. Note the highly ordered EFs arrays and the onionlike structure at the upper right in (B). Scale bar 200 nm.

Table 2: EFs Particle Analysis in Thylakoids from Low-Light- and Ordinary-Light-Grown Plants[a]

	no. of analyzed EFs particles	analyzed area (μm^2)	particle density (μm^{-2})	fraction of particles in arrays (%)
LL	3689	2.75	1436 ± 57	22
OL	2560	1.60	1720 ± 63	<2

[a] A total of 22 micrographs for NL thylakoids and 37 for LL thylakoids were analyzed.

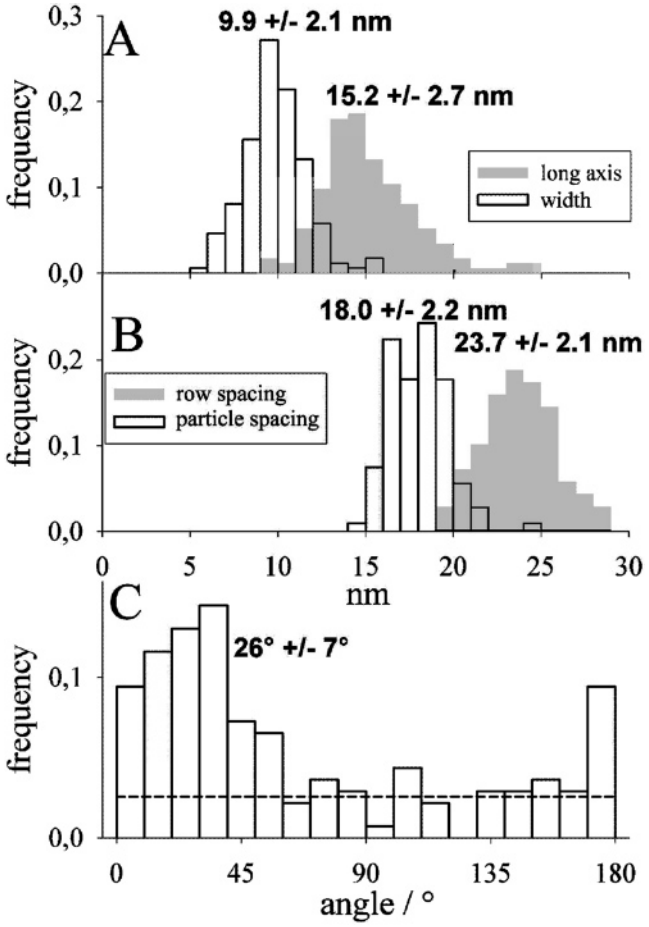

FIGURE 2: Statistical analysis of the EFs particle size, spacing, and orientation in 2D ordered arrays. The dashed line in (C) indicates the expected frequency for a pure random angle distribution. For the long axis and width 173 particles, for the particle spacing 107 particles, for the row spacing 63 rows, and for the angle 138 particles were analyzed.

ordered arrays of EFs particles in thylakoids from low-light-adapted plants (Figure 1B).

Analysis of EFs Particles in Ordered Arrays in Thylakoids from LL-Adapted Plants. In thylakoid membranes isolated from low-light-adapted plants about 22% of the EFs particles are organized in ordered arrays which are almost absent in thylakoids from plants grown under OL conditions (Table 2). Typically EFs particles in 2D arrays were arranged in one to three parallel rows (Figure 1B). It is noteworthy that the occurrence of ordered EFs arrays is accompanied by an onionlike arrangement of tubular structures (Figure 1B). These structures represent very likely cylindrical inverted micelles (HII phase) of the lipid MGDG (*17*). No HII phase was observed in thylakoids from OL-adapted plants. For a deeper analysis of the ordered EFs arrays the particles were fitted with a particle count program (OPTMAS 6.5) assuming an elliptical shape (*16*). The results of the fitting are summarized in Figure 2. The lateral dimensions of the particles deduced from the histogram in Figure 2A (15.2 nm × 9.9 nm) are in agreement with published values for EFs particles (*16*). Furthermore, the distance between two adjacent particles within the same row (18.0 nm), the spacing between two rows (23.7 nm), and the angle between the long axis of an EFs particle and the axis of the row (26°) are in good accordance with literature data on 2D EFs arrays (*18*, *19*). An important question was whether the gaps between adjacent EFs particles localized in the same row are filled with protein complexes (e.g., LHCII trimers or cytochrome b_6f complexes). From inspection of PF micrographs which show grooves corresponding to EFs particles organized in 2D arrays (*18*), it seems that the grooves are totally devoid of particles (Figure 3), indicating the absence of protein complexes between neighboring EFs particles. Although the micrograph suggests that there is no mass within the grooves, the resolution of the micrograph is too low to rule out the possibility that there are small proteins (i.e., monomeric LHCII) present.

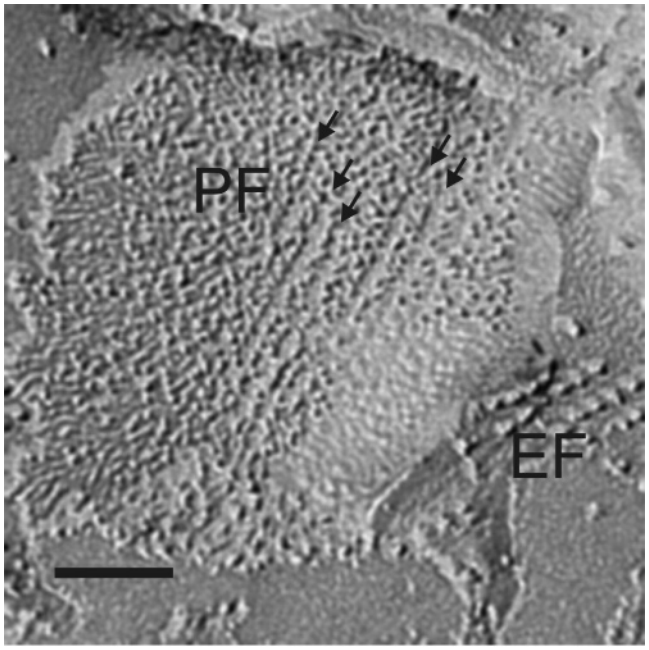

FIGURE 3: PF fracture face from LL thylakoid membranes. Note the grooves in the PF face (indicated by arrows). The distance between the center of a groove and the center of the neighboring groove is between 20 and 25 nm, which corresponds to the spacing of the EFs rows (Figure 1B). Scale bar 100 nm.

Chlorophyll a Fluorescence Induction. Figure 4 shows examples for induction kinetics of the variable chlorophyll *a* fluorescence (F_v) in the presence of DCMU, reflecting the

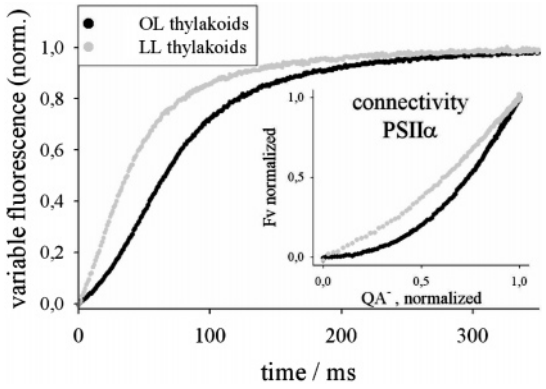

FIGURE 4: Chlorophyll *a* fluorescence induction kinetics of isolated thylakoids from LL and OL plants. The normalized variable parts of chlorophyll *a* fluorescence (F_v) are shown. Kinetics were recorded in the presence of 20 μM DCMU. Inset: Connectivity plot for PSIIα. The normalized area growth of the F_v transient (deduced from the analysis described in ref *20*) reflecting the fraction of QA^- (*x* axis) is plotted versus F_v. The higher the deviation from linearity, the higher the connectivity. F_v/F_0 ratios were 3.2 ± 0.1 for OL and 1.6 ± 0.1 for LL samples.

light-induced reduction of QA. Although the actinic light intensity is the same (starting at 0 ms), the curve for thylakoids isolated from LL-grown plants is significantly faster and less sigmoid compared to that for OL thylakoids. Extracting quantitative parameters from F_v kinetics in the presence of DCMU can be done either by a method established in ref *20* or by a more recently developed procedure which includes various models for excitonic connectivity (*21*). Both models assume a PSIIα/PSIIβ heterogeneity (*22*). Compared to β-type centers, α-centers have a 2−3-fold larger antenna size and are in excitonic contact (connectivity); i.e., excitons are shared among several reaction centers via connected antenna chlorophylls. Table 3 summarizes the results of both methods, which gave almost identical values. The data indicate that in thylakoids isolated from LL-adapted plants the antenna sizes of PSIIα and PSIIβ centers are about 55−60% and 5−14% larger, respectively. Furthermore, the fraction of fluorescence emitted by β-type PSII centers is almost unchanged, whereas the connectivity parameter for PSIIα decreases significantly (see also the inset in Figure 4).

DISCUSSION

Stoichiometries and Antenna Sizes. The data in Table 1 clearly indicate a remodeling of the photosynthetic machinery in grana membranes of LL-adapted plants. To translate the changes in Chl *a*/*b* ratios and marker redox chromophores in protein complex concentrations, Table 4 was generated. For these calculations we neglect smaller PSII complexes (e.g., CP43-free PSII complexes) which may reflect a population of photosystems involved in the repair cycle (*23*). It is reasonable to neglect this population because their abundance in grana regions is rather low (about 5%; *23*). An alternative calculation on the same type of grana vesicles but using an estimation of PSII (signal II, YD) and PSI (P700) from EPR (*23*) and different assumptions is presented in Table 5. This gives an estimate of the number of LHCII trimers per PSII in the intact appressed grana membrane in the same way as shown in Table 4. The antenna sizes, i.e., number of chlorophyll molecules per PSII, given in Table 5 are larger than those given in Table 4. This is partly due to the EPR method, which gives lower values for PSII than those obtained for cytochrome b_{559} given in Table 4. The *relative* changes induced by low light are, however, the same for the two alternative calculations.

The data in Tables 4 and 5 show that low photon flux densities induced a significant increase in the LHCII/PSII ratio, showing that chlorophylls were redistributed from LHCII−PSII supercomplexes to LHCII whereas the chlorophyll contribution from PSI was almost constant (see the percentages in Table 4 and 5). Thus, the redistributions occurred only in the central appressed core of the grana and not in the peripheral stroma exposed margins.

The changes in the LHCII/PSII stoichiometry were accompanied by a decrease in the EFs particle density in electron micrographs of freeze-fractured thylakoids (Table 2), indicating a decreased PSII and an increased LHCII abundance in LL grana membranes. From the EFs densities and the calculated LHCII trimer/PSII ratios (Table 4 or 5), one can estimate that the mean LHCII density was increased by about 40% in LL grana thylakoids compared to their OL counterparts ($1436 \times 5.42/(1720 \times 3.28)$). This redistribution of chlorophylls is accompanied by an about 55−60% increase in the functional antenna size of PSIIα centers in low-light-grown plants concluded from fluorescence induction measurements (Figure 4, Table 3). This is roughly in agreement with the calculated 44−46% increase in the PSII antenna size taking the sum of chlorophylls from LHCII and PSII in LL and OL grana thylakoids, as shown in Tables 4 and 5, suggesting that almost all LHCIIs are functionally connected to PSII. In addition to the functional chlorophyll redistribution in the antenna system of PSII, the mean density of the cytochrome b_6f complex decreased in LL grana thylakoids. From the EFs densities (Table 2) and protein

Table 3: Analysis of Chlorophyll *a* Fluorescence Induction Curves[a]

	k_α (antenna size of PSIIα) (s^{-1})	k_β (antenna size of PSIIβ) (s^{-1})	$F_{v,\beta}$	connectivity of PSIIα
OL thylakoids	14.6 ± 0.8 (15.2 ± 0.7)	7.0 ± 1.2 (7.5 ± 1.0)	0.36 ± 0.01	1.75 ± 0.13
LL thylakoids	23.1 ± 1.7 (23.6 ± 1.1)	8.0 ± 0.9 (7.9 ± 0.6)	0.27 ± 0.03	0.68 ± 0.10
LL/OL ratio	1.58 (1.55)	1.14 (1.05)	0.75	0.39

[a] The curves were analyzed according to the method based on the exciton−radical pair theory (*21*) or the method introduced in ref *20*. The results from the latter analysis are given in parentheses. The numbers are the means of three independent determinations with the standard deviation. $F_{v,\beta}$ is the fraction of fluorescence emitted by PSIIβ centers. The connectivity parameter was deduced from the fitting of PSIIα fluorescence according to ref *21*. The light intensity for chlorophyll excitation was the same in all experiments.

Table 4: Calculation of Protein Complex Concentrations in Grana Thylakoids on a PSII Basis[a]

	LL grana	OL grana	LL/OL
PSII complex (monomeric, without LHCII), set as 1.00	1.00 (20%)	1.00 (29%)	
LHCII−PSII supercomplex (dimeric)	0.50 (33%)	0.50 (48%)	
LHCII trimer (total)	5.42 (70%)	3.28 (61%)	1.65
LHCII trimer (not bound in LHCII−PSII supercomplexes)	4.42 (57%)	2.28 (42%)	
PSI (including four LHCIs)	0.19 (10%)	0.14 (10%)	
cytochrome b_6f complex	0.32	0.35	
antenna size of PSII 66 + 5.42 × 42 (LL); 66 + 2.59 × 42 (OL) (number of chlorophyll molecules/PSII)	294	204	1.44

[a] It is assumed that (i) the PSII complex contains 66 chlorophylls (108 for the LHCII−PSII supercomplex (*27*), minus 42 for one LHCII trimer (*45*), (ii) each LHCII trimer binds 42 chlorophylls (*45*), and (iii) each PSI complex binds 4 LHCIs, which sums up to 167 chlorophylls (*46*). On the basis of these assumptions, the PSII/chlorophyll ratio (c_{PSII}) is given by $c_{PSII} = 1/[66 + c_{LHCII}/c_{PSII} \times 42 + c_{PSI}/c_{PSII} \times 167]$. c_{LHCII}/c_{PSII} (total LHCII trimer in the table) was calculated by solving this equation and taking the data for c_{PSII} and c_{PSI} from Table 1. The data are expressed relative to the PSII concentration (set as 1). Percentage values in parentheses give the chlorophyll fraction bound to the complexes calculated from c_{PSII}, c_{PSI}, c_{LHCII}, and the chlorophyll/complex ratios given above. Italic numbers indicate an organization in dimeric LHCII−PSII supercomplexes.

Table 5: Calculation of Protein Complex Concentrations in Grana Thylakoids Based on EPR Quantifications and Assuming That PSI in Grana Has a 40% Larger Antenna than Stroma Lamellae (*47*)[a]

	LL grana	OL grana	LL/OL
PSII (monomeric, without LHCII), set as 1.00	1.00 (17%)	1.00 (25%)	
LHCII trimer (total connected to PSII)	7.1 (57%)	4.2 (48%)	1.69
PSI (including four LHCIs and LHCIIs connected to PSI)	0.58 (26%)	0.42 (27%)	
antenna size of PSII (number of chlorophyll molecules/PSII)	388	266	1.46

[a] Assumptions: (i) PSII without LHCII trimer binds 90 chlorophylls (*48*). (ii) Each LHCII trimer binds 42 chlorophylls (Table 4). (iii) Each grana PSI complex (PSIα) has a 40% larger antenna than PSIβ (set as 167; see Table 4), i.e., 1.4 × 167 = 234 Chl's/PSIα. The same equation as in Table 4 was used for calculating the LHCII/PSII stoichiometry. The PSII concentration for OL and LL is 2.74 and 1.91 mmol/mol of Chl, respectively. The OL value 2.74 is from ref *11*, and the LL value is obtained by multiplying the 2.74 by the ratio LL/OL (3.07/4.41) for cytochrome b_{559} of grana (Table 1). The PSI concentration for OL and LL is 1.14 and 1.10 mmol/mol of Chl, respectively. The OL value 1.14 comes from ref *11*, and the LL value is obtained by multiplying it by 0.59/0.61, the LL/OL ratio from Table 1. The chlorophyll values in ref *11*, determined by the Arnon method, have been converted to values according to the method of Porra; see ref *11*. Percentage values in parentheses as in Table 4.

ratios in Table 4 it follows that the cytochrome b_6f particle density decreased by about 24% (1436 × 0.32/(1720 × 0.35)). In summary, the remodeling in grana thylakoids of low-light-adapted plants indicates an enhanced light-harvesting function (LHCII) and a decreased electron-transport function (PSII and cytochrome b_6f complex) as was proposed in the literature (e.g., refs *1* and *8*). This could be a strategy for an economic utilization of limited resources (light energy, amino acids, cofactors) under low photon flux densities.

Ordered PSII Arrays: Effect on Plastoquinone Mobility. As pointed out above LL-induced remodeling in grana thylakoids leads to a decreased abundance of larger particles (LHCII−PSII supercomplexes, area about 220 nm^2; *12*) and an increase of smaller particles (LHCII trimers, area about 34 nm^2; *12*). It is expected that this influences lateral diffusion processes, in particular the migration of plastoquinone from PSII to the cytochrome b_6f complex and *vice versa*. Grana thylakoids are crowded by integral protein complexes (*24*) which act as diffusion obstacles (*24*, *25*). With the same area occupation diffusion is more hindered in membranes with smaller obstacles compared with membranes with larger particles as shown by computer simulations (*25*, *26*). Furthermore, the efficiency of PQ diffusion seems to be at its limit in OL-grown plants due to molecular crowding (*25*). Slight changes in the protein arrangement and density lead to pronounced effects on lateral plastoquinone mobility (*25*). Thus, it is expected that the increase in density of (smaller) LHCII complexes and the fact that the mean diffusion path for PQ between PSII and cytochrome b_6f complexes is increased in LL grana thylakoids due to dilution of these protein complexes (Table 1) cause serious problems for finding the binding niches by random migration. We propose that supramolecular ordering of protein complexes is a strategy to overcome these potential diffusion problems in crowded membranes. Evidence has been presented that the protein complexes in grana thylakoids are not randomly distributed but form ordered, local arrangements which might optimize lateral diffusion (*24*). In this respect the occurrence of ordered PSII arrays in LL-adapted plants which were almost absent in their OL-grown counterparts (Figure 1, Table 2) is interesting. To visualize the organization of complete LHCII−PSII supercomplexes in these arrays, known supercomplex structures were modeled in the EFs arrays (Figure 5). It is assumed that the EFs particles represent a PSII core dimer which may or may not bind minor LHCII complexes (*16*). Furthermore, the position and orientation of the dimeric PSII core within the super-

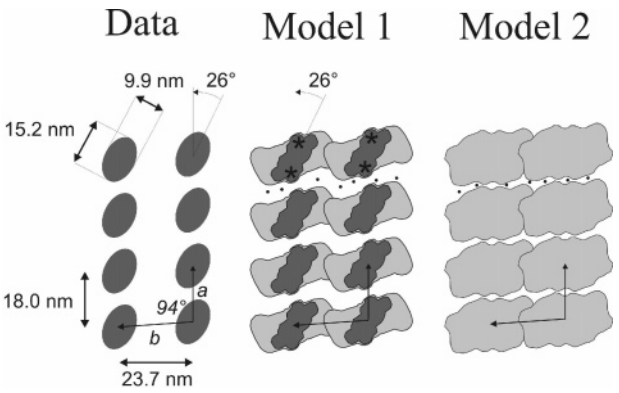

FIGURE 5: (Left) Summary of the organization of the EFs particles in 2D arrays. (Middle and right) Models of the supercomplex arrangement. The contour of the supercomplex and the positioning of the PSII core dimer (dark gray) in model 1 were taken from ref *27*. The contour for the model was from ref *29*. Asterisks mark the position of the QB binding pocket. The small black circle in the models represents the size of PQ.

complex are known (*9*, *27*). On the basis of these findings, models 1 and 2 in Figure 5 were generated. Because only medium-resolution structures of the supercomplex are available, there is some degree of uncertainty in the overall shape. We therefore model two extreme cases of published structures (Figure 5). Support for these models comes from the observation that probably no proteins (i.e., LHCII trimers) are between neighboring EFs particles localized in the same row (Figure 3) as predicted by Figure 5. The models predict that two adjacent supercomplexes in neighboring rows share one LHCII trimer (the overlap in Figure 5). Noteworthy is that similar particles (dimers of supercomplexes) were recently isolated after mild solubilization of *Chlamydomonas* thylakoids (*9*). A number of EM data on PSII arrays with higher resolution were published for detergent-solubilized membranes (e.g., refs *28* and *29*). These data suggest that there is hardly any protein-free space between PSII rows. Detailed comparisons of our data with the published arrangements reveal slight differences concerning the spacing and angles of supercomplexes in ordered arrays (not shown). These differences seem to be important because they determine whether a lipidic gap is formed between PSII rows (Figure 5) (*28*, *29*). A possible explanation for these differences could be that in refs *28* and *29* detergent-solubilized membranes were examined, which could induce slight changes in the PSII arrangement. In this respect it is of note that photosynthetic membrane protein complexes show a differential solubilization tendency. E.g., for the isolation of cytochrome b_6f complexes from thylakoids the detergent concentration can be adjusted to selectively extract b_6f complexes but to leave chlorophyll protein complexes in the membrane (*30*).

Concerning the potential problems with PQ diffusion in grana thylakoids from LL plants (see above), the proposed models have interesting features. Reduced PQ released from the QB binding niche (marked by asterisks) would migrate in a kind of lipidic diffusion channel (in the horizontal direction). The vertical direction is blocked by overlapping LHCII trimers. As a consequence PQ diffusion would switch from a two-dimensional to a kind of one-dimensional process, which, according to the Einstein equation, lowers the diffusion times. Furthermore, the organization in Figure 5 ensures that the QB binding niche is not blocked by proteins due to a spacing of supercomplexes. Thus, the arrangement of the PSII complex in 2D arrays in the LL grana membrane could be a strategy to overcome potential problems with PQ diffusion which arose from a tighter packing of (smaller) LHCII complexes. An attractive speculation is that cytochrome b_6f complexes are associated with ordered PSII rows. For example, it could be that this complex is localized in or at the end of the PQ diffusion "channel". This arrangement would ensure a very efficient functional connection of PSII and Cyt b_6f complexes. However, at the moment there is no evidence for or against this model. An uncertainty with the models in Figure 5 is the question of whether the lipidic areas between the rows are completely protein free. The uncertainty results from the low resolution in the PF micrographs. In ref *31* the quality of micrographs showing PF grooves corresponding to ordered EF arrays was better. These images support our suggestion. However, further studies are necessary to answer this question.

As a consequence of the higher LHCII and lower PSII density in LL grana thylakoids the mean separation between neighboring photosystems should be larger. It is noteworthy that the density of 1436 EFs's/μm^{-2} is a mean value of semicrystalline and noncrystalline areas. Because the density in the ordered regions is larger (about 2380 EFs's/μm^{-2}, calculated from Figure 5, left), the density in the 2D array free EFs areas is still lower. Assuming that 22% of the EFs particles are organized in 2D arrays (Table 2), a value of 1170 EFs's/μm^{-2} can be calculated for noncrystalline areas ($(1436 - 2380 \times 0.22)/0.78$). Thus, in these regions PSII is about one-third diluted in LL grana thylakoids compared to OL membranes (1170/1720), indicating an increased separation. Because the apparent antenna size of PSIIα was increased (Table 3) and the LHCII/PSII ratio raised (Tables 4 and 5) in LL thylakoids, it is likely that additional LHCII complexes were arranged between neighboring PSII complexes in noncrystalline regions of grana thylakoids. This could be the reason for the decreased connectivity between PSIIα centers in thylakoids isolated from plants grown under low light (Table 3 and inset in Figure 4). Evidence has been presented that the lateral diffusion radius for excitonic energy migration in grana membranes (which require both intra- and intermolecular energy transfer) is limited to a few tens of nanometers (*32*). Thus, the probability for the transfer of excitons from a given photosystem to its neighbors decreases with an increase in distance. Following this interpretation would imply that the connectivity between PSIIα centers decreases with increasing antenna size (see Figure 4) as should be realized in nonordered regions in LL grana membranes but not in ordered regions.

Nonbilayer HII Phase and Membrane Pressure. In parallel to 2D ordered EFs arrays the nonbilayer HII phase of MGDG in thylakoids occurred (Figure 1B) which was absent in OL-grown plants. This suggests that both phenomena are affiliated with each other as was already supposed (*19*, *31*). It is noteworthy that MGDG in the HII phase does not contribute to the membrane bilayer phase. Furthermore, it was reported that growing squash in LL did not significantly alter the lipid content and composition in thylakoid membranes compared to OL plants (*33*). Combining both observations would mean that HII phase formation has two effects in grana membranes of LL plants. First, the protein density in the membrane bilayer increases (fewer lipids in the bilayer). This implies that potential PQ diffusion problems as mentioned above could be intensified by HII phase formation. Second, the ratio of non-bilayer-forming to bilayer-forming lipids decreases within the membrane bilayer. It is expected that this has consequences on the lateral pressure in membranes. Due to its cone shape MGDG intrinsically has a high tendency to from concave half-membranes (*17*). Forcing MGDG in a bilayer generates a physical "frustration" which causes a lateral pressure in the hydrophobic core of the membrane (*34*). As a fraction of MGDG forms HII phases in LL grana thylakoids, the abundance of this lipid in the bilayer phase decreases and the lateral membrane pressure should be lower compared to that of OL plants. One can speculate that decreasing the membrane pressure causes an alteration in the binding properties of trimeric LHCII to PSII supercomplexes, leading to its unbinding. This could trigger the reorganization of PSII supercomplexes into 2D semicrystalline arrays. Interestingly,

decreasing the level of unsaturation of thylakoid fatty acids leads to a dissociation of LHCII form PSII (*35*). Noteworthy, it is expected that this treatment causes a decrease of lateral membrane pressure (*36*). It has been suggested that the thylakoid bilayer structure is stabilized not only by the membrane proteins but also by carotenoids. There is strong evidence that most of the xanthophylls (violaxanthin, zeaxanthin, and antheraxanthin) are free in the lipid phase (*37*, *38*), and it has been suggested that these stabilize the bilayer structure (*39*−*41*). The amount of xanthophylls decreases with low irradiation during growth (*42*), which means that there are fewer xanthophylls in our low-light vesicles and hence there is less stabilization. This could be the primary reason for formation of HII phases, in our LL grana thylakoids, followed by less space for proteins and an decrease in lateral pressure. Furthermore, the MGDG to total lipid ratio decreases in cold- or salt-stressed plants (*43*, *44*), indicating that the lateral membrane pressure could be of physiological significance. It seems that stress in general induces HII phase formation, so one might conclude that very low light is a stress factor. However, further studies are necessary to understand the relationship between membrane pressure and protein organization in thylakoids.

This study shows that growing plants under low photon flux densities leads to a remodeling of the protein complex composition which improves the light-harvesting function. This was accompanied by a lateral segregation in grana thylakoids: Highly ordered semicrystalline PSII arrays occurred in the same membrane patch with unordered regions. Probably this rearrangement could be a response to potential lateral diffusion problems associated with the increased abundance of smaller LHCII complexes and the dilution of PSII and cytochrome b_6f complexes.

ACKNOWLEDGMENT

Ricarda Höhner (Institute of Botany, Münster) is acknowledged for her help with chlorophyll fluorescence measurements and Hans-Erik Åkerlund (Department of Biochemistry, Lund University) for stimulating discussions on the role of xanthophylls in the membrane bilayer structure.

REFERENCES

1. Anderson, J. M. (1986) Photoregulation of the composition, function, and structure of thylakoid membranes, *Annu. Rev. Plant Physiol. 37*, 93−136.
2. Walters, R. G. (2005) Towards an understanding of photosynthetic acclimation, *J. Exp. Bot. 56*, 435−447.
3. Mustardy, L., and Garab, G. (2003) Granum revisited. A three-dimensional model−where things fall into place, *Trends Plant Sci. 8*, 117−122.
4. Nelson, N, and Ben-Shem, A. (2004) The complex architecture of oxygenic photosynthesis, *Nat. Rev. Mol. Cell Biol. 5*, 1−12.
5. Albertsson, P.-A. (2001) A quantitative model of the domain structure of the photosynthetic membrane, *Trends Plant Sci. 6*, 349−354.
6. Blankenship E. B. (2002) *Molecular mechanisms of photosynthesis*, Blackwell Science, Oxford, U.K.
7. Anderson, J. M. (1988) Thylakoid membrane organisation in sun/shade acclimation, *Aust. J. Plant Physiol. 15*, 11−26.
8. Albertsson, P.-A., and Andreasson, E. (2004) The constant proportion of grana and stroma lamellae in plant chloroplast, *Physiol. Plant. 121*, 334−342.
9. Dekker, J. P., and Boekema, E. J. (2005) Supramolecular organization of thylakoid membrane proteins in green plants, *Biochim. Biophys. Acta 1706*, 12−39.
10. Andreasson, E., Svensson, P., Weibull, C., and Albertsson, P. Å.-(1988) Separation and characterization of stroma and grana membranes−evidence for heterogeneity in antenna size of both photosystem I and photosystem II, *Biochim. Biophys. Acta 936*, 339−350.
11. Danielsson, R., Albertsson, P. Å., Mamedov, F., and Styring, S. (2004) Quantification of photosystem I and II in different parts of the thylakoid membrane from spinach, *Biochim. Biophys. Acta 1608*, 53−61.
12. Kirchhoff, H., Mukherjee, U., and Galla, H.-J. (2002) Molecular architecture of the thylakoid membrane: Lipid diffusion space for plastoquinone, *Biochemistry 41*, 4872−4882.
13. Kaminskaya, O., Kern, J., Shuvalov, V. A., and Renger, G. (2005) Extinction coefficients of cytochromes b559 and c560 of Thermosynechococcus elongates and Cyt b559/PSII stoichiometry of higher plants, *Biochim. Biophys. Acta 1708*, 333−341.
14. Schöttler, M. A., Kirchhoff, H., and Weis, E. (2004) Photosynthetic electron transport to the carbon metabolism in tobacco, *Plant Physiol. 136*, 4265−4274.
15. Kirchhoff, H., Borinski, M., Lenhert, S., Chi, L., and Büchel, C. (2004) Transversal and lateral exciton energy transfer in grana thylakoids of spinach, *Biochemistry 43*, 14508−14516.
16. Staehelin, L. A., and van der Staay G. W. M. (1996) Structure, composition, functional organization and dynamic properties of thylakoid membranes, in *Oxygenic photosynthesis: The light reactions* (Ort, D. A., and Yocum C. F., Eds.) pp 11−30. Kluwer Academic Publishers, Dordrecht, The Netherlands.
17. Williams, W. P. (1998) The physical properties of thylakoid membrane lipids and their relation to photosynthesis, in *Lipids in photosynthesis: Structure, function and genetic*s (Siegenthaler, P.-A., and Murata, N., Eds.) pp 145−173, Kluwer Academic Publishers, Dordrecht, The Netherlands.
18. Simpson, D. J. (1978) Freeze-fracture studies on barley plastid membranes II: Wild-type chloroplast, *Carlsberg Res. Commun. 43*, 365−389.
19. Tsevtkova, M, N., Apostolova, E. L., Brain, A. P. R., Williams, W. P., and Quinn, P. J. (1995) Factors influencing PSII particle array formation in Arabidopsis thaliana chloroplasts and the relationship of such arrays to the thermostability of PSII, *Biochim. Biophys. Acta 1228*, 201−210.
20. Melis, A., and Homann, P. H. (1976) Heterogeneity of the photochemical centers in system II of chloroplasts, *Photochem. Photobiol. 23*, 343−350.
21. Lavergne, J., and Trissl, H.-W. (1995) Theory of fluorescence induction in photosystem II: Derivation of analytical expressions in a model including exction-radical-pair equilibrium and restricted energy transfer between photosynthetic units, *Biophys. J. 68*, 2474−2492.
22. Lavergne, J., and Briantais, J.-M. (1996) Photosystem II heterogeneity, in *Oxygenic photosynthesis: The light reactions* (Ort, D. A., and Yocum, C. F., Eds.) pp 265−287, Kluwer Academic Publishers, Dordrecht, The Netherlands.
23. Danielsson, R., Suorsa, M., Paakkarinen, V., Albertsson, P. A., Styring, S., Aro, E. M., and Mamedov, F. (2006) Dimeric and monomeric organization of photosystem II. Distribution of five distinct complexes in the different domains of the thylakoid membrane, *J. Biol. Chem. 281*, 14241−14249.
24. Kirchhoff, H., Tremmel, I., Haase, W., and Kubitscheck, U. (2004) Supramolecular photosystem II organization in grana thylakoid membranes: evidence for a structured arrangement, *Biochemistry 43*, 9204−0213.
25. Tremmel, I. G., Kirchhoff, H., Weis, E., and Farquhar, G. D. (2003) Dependence of plastoquinol diffusion on the shape, size, and density of integral thylakoid proteins, *Biochim. Biophys. Acta 1607*, 97−109.
26. Saxton, M. J. (1989) Lateral diffusion in an archipelago. Distance dependence of the diffusion coefficient, *Biophys. J. 56*, 615−622.
27. Hankamer, B., Nield, J., Zheleva, D., Boekema, E., Jansson, S., and Barber, J. (1997) Isolation and biochemical characterization of monomeric and dimeric photosystem II complexes from spinach and their relevance to the organisation of photosystem II *in vivo*, *Eur. J. Biochem. 243*, 422−429.
28. Boekema, E. J., van Breemen, J. F. L., van Roon, H., and Dekker, J. P. (2000) Arrangement of photosystem II supercomplexes in crystalline macrodomains within the thylakoid membrane of green plant chloroplast, *J. Mol. Biol. 301*, 1123−1133.
29. Morosinotto, T., Bassi, R., Frigerio, S., Finazzi, G., Morris, E., and Barber, J. (2006) Biochemical and structural analyses of higher

plant photosystem II supercomplex of photosystem I-less mutant of barley, *FEBS J. 273*, 4616−4630.
30. Hauska, G. (2004) The isolation of a functional cytochrome b_6f complex: from lucky encounter to rewarding experiences, *Photosynth. Res. 80*, 277−291.
31. Semenova, G. A. (1995) Particle regulartiy on thylakoid fracture faces is influenced by storage conditions, *Can. J. Bot. 73*, 1676−1682.
32. Barzda, V., Garab, G., Gulbinas, V., and Valkunas, L. (1996) Evidence for long-range excitation energy migration in macroaggregates of the chlorophyll a/b light harvesting antenna complexes, *Biochim. Biophys. Acta 1273*, 231−236.
33. Xu, Y., and Siegenthaler, P.-A. (1996) Effect on non-chilling temperature and light intensity during growth of squash cotyledons on the composition of thylakoid membrane lipids and fatty acids, *Plant Cell Physiol. 37*, 471−479.
34. Van den Brinck-van der Laan, E., and Killian, J. A., de Kruijff, B. (2004) Nonbilayer lipids affect peripheral and integral membrane proteins via changes in the lateral pressure profile, *Biochim. Biophys. Acta 1666*, 275−288.
35. Horvath, G., Melis, A., Hideg, E., Droppa, M., and Vigh, L. (1987) Role of lipids in the organization and function of photosystem II studied by homogeneous catalytic hydrogenation of thylakoid membranes in situ, *Biochim. Biophys. Acta 891*, 68−74.
36. Bishop, D. G., Kenrick, J. R., Bayston, J. H., MacPherson, A. S., and Johns, S. R. (1980) Monolayer properties of chloroplast lipids, *Biochim. Biophys. Acta 602*, 248−259.
37. Arvidsson, P. O., Carlsson, M., Steffánsson, H., Albertsson, P.-Å., and Åkerlund, H.-E. (1997) Violaxanthin accessibility and temperature dependency for de-epoxidation in spinach thylakoid membranes, *Photosynth. Res. 52*, 39−48.
38. Eskling, M., and Åkerlund, H-E. (1998) Time course of changes in the quantities of violaxanthin de-epoxidase, xanthophylls and ascorbate in spinach upon shift from low to high light, *Photosynth. Res. 57*, 41−50.
39. Gruszecki, W. I., and Strzalka, K. (2005) Carotenoids as modulators of lipid membrane physicalproperties, *Biochim. Biophys. Acta 1740*, 108−115.
40. Gruszecki, W. I., and Strzalka, K. (1991) Does the xanthophyll cycle take part in the regulation of fluidity of the thylakoid membrane? *Biochim. Biophys. Acta 1060*, 310−314.
41. Szilágyi, A., and Åkerlund, H.-E. (2007) Laurdan fluorescence spectroscopy in the thylakoid bilayer: the effect of violaxanthin to zeaxanthin conversion on the galactolipid dominated lipid environment, in Xanthophyll cycle in the light of thylakoids membrane lipids. Membrane packing, curvature elastic stress and enzyme binding, Thesis, Lund University.
42. Thayer, S. S., and Björkman, O. (1990) Leaf xanthophyll content and composition in sun and shade determined by HPLC, *Photosynth. Res. 23*, 331−343.
43. Harwood, L. (1998) Involvement of chloroplast lipids in the reaction of plants submitted to stress, in *Lipids in Photosynthesis: Structure, function and genetics* (Siegenthaler, P. A., and Murata, N., Eds.) pp 290−300, Kluwer Academic Publishers, Dordrecht, The Netherlands.
44. Gigon, A., Matos, A. R., Laffray, D., Zuil-Fodil, Y., and Pham-Ti, A. T. (2004) Effect of drought stress on lipid metabolism in the leaves of Arabidosis thaliana, *Ann. Bot. (London) 94*, 345−351.
45. Liu, Z., Yan, H., Wang, K., Kuang, T., Zhang, J., Gui, L., An, X., and Chang, W. (2004) Crystal structure of spinach major light-harvesting complex at 2.72 A resolution, *Nature 428*, 287−292.
46. Ben-Shem, A., Frolow, F., and Nelson, N. (2003) Crystal structure of plant photosystem I, *Nature 426*, 630−635.
47. Svensson, P., Andreasson, E., and Albertsson, P. Å.(1991) Heterogeneity among Photosystem I, *Biochim. Biophys. Acta 1060*, 45−50.
48. Jansson, S. (1994) The light harvesting chlorophyll a/b-binding proteins, *Biochim. Biophys. Acta 1184*,1−19.

BI700748Y